WEST VIRGINIA UNIVERSITY

PLASMA PHYSICS GROUP

INTERNAL REPORT PL - 046

Spectroscopy System and Basic Spectroscopy
Diagnostics for the HELIX and LEIA Plasma Devices

R.F. Boivin

December 2000

TABLE OF CONTENT

1.0 Spectroscopy system/Definitions

The spectroscopy system is composed of many components. A brief description of the different components of the spectrometer is given in this document. For additional information, the reader should consult the following references [1-5]. The different terms, definitions and, concepts applied in the field of spectroscopy are also concisely discussed.

Spectrometer: Class of instruments that collects, spectrally disperses, and re-images an optical signal. The output signal is a series of monochromatic images corresponding to the wavelengths present in the incident light at the entrance slit. A spectrometer is designed to measure the distribution of radiation from a source in a specific wavelength region. Its principal components are a monochromator and a radiant detector. A spectrometer is composed of the following:

1) An entrance slit or aperture.
2) A collimating element to make parallel all rays that just came through the entrance slit. This collimator may be a lens, a mirror or a part of the dispersing element
3) A dispersing element, which spreads the light as function of wavelength.
4) A focusing element to form an image at the exit slit or at the field-stop at some convenient focal plane. The image is formed at the exit slit of the monochromator or at the detector focal plane of the spectrograph.
5) An exit slit or field stop at the focal plane. For a multi-channel detector system (spectrograph configuration) the detector forms the exit field stop.
6) A radiant detector such as a photomultiplier tube or a multi-channel detector (photodiode array or CCD camera).

Monochromator: Essential component of the spectrometer that forms an image of the entrance slit in the exit plan at the wavelength present in the light source. It can be either manually tuned, presenting one wavelength (or wavelength interval) at a time at the exit slit, or motorized, presenting a sequential scan of a wavelength range (scanning monochromator). The monochromator selects a narrow spectral band of radiant power and transmits it through the exit slit to the photosensitive surface of the detector. In a spectrograph configuration, the exit slit is removed and, the dispersed spectrum is distributed across the photosensitive surface of a multi-channel detector. The monochromator can be used for two distinct applications; first, as a filter where the monochromator select a narrow portion of the spectrum enabling irradiation of a sample. Second and foremost, as a spectral analysis tool where a photosensitive detector is placed on the exit slit to detect the different components of any emitting source. A monochromator is characterized by the following parameters:

1) Type
2) Spectral range
3) Focal length
4) f - number and numerical aperture
5) Solid angle
6) Etendue
7) Grating
8) Angular dispersion
9) Linear dispersion
10) Resolution
11) Bandwidth
12) Stay light
13) Slit configuration
14) Display / precision / scanning

Monochromator type: There are numerous configurations of monochromator available on the market. The principals optical systems used are Czerny-Turner, Crossed Czerny-Turner, Ebert-

Fastie, Rowland and Seya-Namoya. The Czerny-Turner optical system, which used a plane grating with focusing mirrors, is found in most air-path monochromators (see Figure 1). It consists of two concave mirrors and one plane diffraction grating. The incident light enters the monochromator through the entrance slit. The light is then focused and collimated by the concave mirror on the dispersing element (grating). The grating spreads the light as a function of wavelength (same function as a prism). The second concave mirror collimates and focuses a selected wavelength interval on the exit slit or the exit field stop (spectrograph mode). Two lateral folding mirrors near the entrance and exit slits allows the instrument to be used in many configurations. For intense sources, the end-mounted configuration is better suited since the radiation is spread over the entire collimating mirror rather than on a smaller lateral-folding mirror.

Spectral range: The spectral range of monochromators varies greatly from one monochromator to another. Usually a distinction is made between three separate classes of monochromators:

1) UV (Ultraviolet) - VIS (Visible) - IR (Infrared)
2) VUV (Vacuum Ultraviolet)
3) UHV (Ultra High Vacuum)

The UV-VIS-IR class monochromators are the most commonly used. In general, since this type of monochromator features an air pathway, their wavelength range is limited, on the low side, by oxygen absorption at about 185 nm. Limited extension of this range is possible provided the monochromator can be purged for controlled atmosphere (N_2 or any inert gases). The upper limit is usually in the 20 μm range or higher. Usually, the grating used in the monochromator will reduce the spectral range to a fraction of the initial specification. The VUV class of instrument operates in vacuum (10^{-6} Torr). Their spectral range is between 30 nm to 1 μm. The UHV class operates under extreme vacuum (10^{-10} Torr). Their spectral range is typically between 1 nm and 200 nm.

Focal length: Optical path length of the incident light from the entrance slit to the dispersing element.

F - number, numerical aperture: The f-number (also identified as the focal ratio) is a fundamental characteristic of the instrument and cannot be modified. The f-number is a measure of the energy throughput in the monochromator. The lower the number, the higher the energy throughput. As the focal length increase, the f-number proportionally decreases. The numerical aperture is proportional to the inverse square root of the f-number.

Solid angle: The solid angle of a monochromator is defined as the solid angle which light emitted by a source must fall in order to enter the monochromator. This quantity will be discussed in details in the next section

Etendue (geometric etendue): The etendue geometrically characterizes the ability of an optical system to accept light. It is a function of the area of the emitting source and, a function of the solid angle. This quantity will be discussed in details in the next section.

Gratings: The grating is the light dispersing element of the instrument. Plane gratings are used in Czerny-Turner monochromators. Their groove density (gr/mm) characterizes them. The higher the density, the larger the angular dispersion and the smaller the linear dispersion. Thus, a high-density grating will finely resolve the spectral composition of the incident light. Adversely, the higher the groove density, the smaller the wavelength interval at the exit aperture stop. There are 3 types of gratings: Blazed Holographic Diffraction gratings, Standard Holographic Diffraction gratings and, Ruled Diffraction gratings. The first type are "State of the Art" and are characterized by the absence of "ghosts" because of their holographic groove spacing and by the high efficiency groove profile at a specific wavelength. Groove densities are between 600 and 2400 gr/mm. The second grating type has generally broad responses at the expenses of high peak efficiency. Again, the holographic groove process yields gratings with no ghosts. Groove densities between 600 and 3600 gr/mm are available. Since these gratings can be used on a wider wavelength interval that the previous type, they are the most commonly used for spectroscopy. Finally, the Ruled Diffraction gratings are mechanically grooved and as such are often plagued by periodic errors in the groove spacing. These errors give rise to ghosts or even focused stray light. Since ghosts intensity increases as the square of the groove density, high-density gratings of this type are not commonly used for spectroscopy. However, some of the best low groove density gratings (300 gr/mm or less) on the market are of this type. As in the case of the first type, these gratings are usually design for a limited spectral range.

Angular dispersion: Light is incident on a grating. The angular dispersion of the diffracted light is the ratio of the angular separation between two wavelengths to the differential separation between two wavelengths.

Linear dispersion

The linear dispersion of a grating system is the inverse of the product of the angular dispersion by the effective focal length. It indicates how many nanometers will be found per unit length of the spectrum at the exit plane (usually given in nm/mm at a specific wavelength and with a grating of 1200 gr/mm). Linear dispersion is associated with an instrument's ability to finely resolve the spectral distribution of the incident light. From the linear dispersion and a slit width, one can evaluate the resolution of the instrument.

Resolution: There are a number of parameters that affect the resolution. The intrinsic resolution of the monochromator is directly proportional to each of the 2 following parameters: groove density of the grating and the focal length. Of course, the resulting resolution is also a function of the slit width. For a slit width larger than the diffraction width of the instrument, the product of the linear resolution and the slit width gives the resolution of a monochromator. The resolution of a visible monochromator is usually given at 5000 Å for a 10 μm slit.

Bandwidth: The bandwidth of a monochromator is determined by measuring the broadening of a monochromatic light source (single mode laser) through the monochromator equipped with a specific grating (usually 1200 gr/mm). The measurement is performed for a given set of entrance and exit slit parameters. The laser light is scanned in wavelength around the central wavelength of interest by rotating the grating. The bandwidth of the monochromator is defined as the full width at half maximum (FWHM) of the resulting lineshape assuming a monochromatic light at the entrance.

Stray light: There are two main causes of stray light in a monochromator. First, diffusion of the light by optical components of the monochromator; this diffusion being associated with the presence of imperfectly polished mirrors and also by unwanted scattering from the gratings. Apart from replacing optical components, the experimentalist can do little to reduce this type of stray light. Second, incorrect illumination of the monochromator. It is important to optimize the optical path of the light that enter and exit the monochromator. Optimizing both the entrance and exit slits can significantly reduce this type of stay light in the monochromator.

Slit configuration: A monochromator is equipped with a minimum of two ports or aperture stops. Additional ports increase the flexibility of the instrument (a folding mirror must be added). At the entrance port, a slit is always used. At the exit port, no slit is needed if the monochromator is used in the spectrograph configuration (with an array detector). A slit is needed when a photomultiplier is used as the radiant detector. The slit height will affect the luminosity of the monochromator. The slit width will affect the resolution of the monochromator. When both slits are used, equal openings of entrance and exit slits will provide optimum luminosity for a given resolution.

Display/ Precision/ Scanning: The display indicates the wavelength that will exit the monochromator. This display must be calibrated with an external calibrated light source. The display usually supposed that a grating of 1200 gr/mm acts as the dispersing element. The display must be multiply by 2 when a 2400 gr/mm grating is used. The precision of the display is usually limited by the mechanical precision of the counter. It doesn't reflect the precision of the monochromator. The scanning velocity indicate the possible speed of the scan (in Å / min) with a stepping value in Å associated with each step of the stepping motor.

2.0 Radiation from the plasma

To optimize light input into a spectrometer, we must first consider the scattered radiation from the plasma. In general, radiation from the plasma is collected by some optical system called matching optics, between the source of the light and the entrance port of the spectrometer. Consider the plasma volume shown in Figure 2. We assume that the emitting volume is located in the center of a plasma slab of thickness *2R*. We also assume that the plasma is uniform within the volume. We define *A* as the image of the light limiting aperture *A'* outside the plasma (monochromator entrance slit) and *S* as the area of this slit image (associated with the slit area *S'*). Radiation originating within this volume will reach the light detecting system if it passes through *A*. The power per unit wavelength interval entering the slit image *S* from an elemental ring shaped volume ($d^2V = 2\pi r^2 \sin\varphi \, d\varphi$; see Figure 2) is given by [3]:

$$dP_\lambda = \varepsilon_\lambda \, d^2V \, S \, r^{-2} \cos\varphi \tag{1}$$

where ε_λ is the emissivity of the plasma at a specific wavelength interval. The total power (watt) per unit wavelength entering the light detection unit is obtain by the integration over the double-conical volume shown in Figure 2:

$$P_\lambda = 2 \, \varepsilon_\lambda \, S \int_0^R \int_0^\theta 2\pi \, r^2 r^{-2} \cos\varphi \, \sin\varphi \, d\varphi \, dr = 2 \, \varepsilon_\lambda \, \pi \, R \, S \, \sin^2\theta \tag{2}$$

where q is the angle subtended by the light collection lens at the center of the slab. Replacing the value of the solid angle subtended the slit image ($W = p \sin^2 q$) in equation (2) yields:

$$P_l = 2\ e_l\ R\ S\ W = I_l\ S \tag{3}$$

where I_l is the irradiance per unit wavelength ($I_l = 2\ e_l\ R\ W$; watt per surface unit) of the plasma source that will reach the detection unit. An important feature is that the result (equation 3) is the same as if the radiation was emitted from a volume equal to the slit image surface at mid-plane times the slab thickness. As we can see, the power per unit wavelength can be described by a product of geometric quantities and a emissivity term:

$$P_l = \underbrace{2R}_{\text{Plasma Thickness}} \cdot \underbrace{e_l}_{\text{emissivity term}} \cdot \underbrace{S\ W}_{\text{geometric terms}} = e_l\ V\ W \tag{4}$$

Where V is the plasma volume defined by the optics. The product $S\ W$ is an important parameter of any light collecting system. It is called the geometric etendue or etendue of the optical system.

2.1 Optical and monochromator etendue

The etendue E of any optical system used to collect light in a radiation scattering experiment is given by [1]:

$$E = s\ W = p\ s \sin^2 q \tag{5}$$

where s is the area of the projection of the scattering volume onto a plane perpendicular to the optical axis of the light collection system and, W is the solid angle into which light leaving the source must fall to enter the collecting optics. The etendue geometrically characterizes the ability of an optical system to accept light. For a light collecting system using a lens, the etendue is independent of the lateral magnification factor M of the lens. This is because the solid angle W is proportional to M^{-2} and, s is proportional to M^2. Thus, considering equation (4) and taking in account the etendue definition (equation (5)) the light collecting system etendue is given by:

$$E_o = S\ W = p\ S \sin^2 q \tag{6}$$

where S is the area of the projected image of the monochromator slit in the plasma. If the distance between the plasma and the lens (X) is large compare to the lens dimension then:

$$\sin q = R_L / X \tag{7}$$

where R_L is the radius of the lens. Rewriting equation (6) in terms of X we obtain:

$$E_o = S\ p\ R_L^2 / X^2 = S\ A_L / X^2 \tag{8}$$

where A_L is the area of the lens. Using the thin lens approximation, the slit image area can be related to the slit surface of the monochromator by the expression:

$$S = M^2 S' \tag{9}$$

where M is the magnification factor of the lens. Expressing equation (8) in terms of the monochromator slit area we have:

$$E_o = S' A_L M^2 / X^2 \tag{10}$$

The etendue is now expressed solely in terms of experimental quantities. Let us consider the etendue of the monochromator. For the monochromator, the etendue corresponds to the maximum beam volume that the instrument can accept. The entrance slit limits the angular spread of the light passing through the instrument. Thus, the etendue of the instrument is according to equation (5) given by:

$$E_M = h\, Dx\, p\, \sin^2 q \tag{11}$$

where h and Dx are the entrance slit height and width (in mm), respectively. The solid angle can be written in terms of the f-number of the instrument (see Figure 3). Re-writing equation (11) in terms of the f-number we obtain:

$$E_M = h\, Dx\, p\, (1 + 4f^2)^{-1} \tag{12}$$

When f is large compare to unity (which is the case for most monochromator), the monochromator etendue becomes:

$$E_M = h\, Dx\, p\, (2f)^{-2} = h\, Dx\, p\, (NA)^2 \tag{13}$$

where NA is the numerical aperture of the instrument. Provided the slit width Dx is large enough (larger than the slit width associated with the intrinsic resolution of the instrument) the instrumental bandwidth $D\lambda$ (usually given as a specification) is given by the expression:

$$D\lambda = D\, Dx \tag{14}$$

where D is the linear dispersion of the instrument (also given as a specification). Replacing the slit width value obtain in the last equation in equation (14) the etendue becomes:

$$E_M = h\, D\lambda\, D^{-1}\, p\, (4f)^{-2} = h\, D\lambda\, D^{-1}\, p\, (NA)^2 \tag{15}$$

Which is now expressed in terms that are listed in the manufacturer specifications. The etendue of the monochromator is sometimes expressed in terms of the grating properties. The etendue is then given by the expression:

$$E_M = h\, n\, k\, G_A\, D\lambda / 10^6\, F \tag{16}$$

where n is the grating groove density, k the diffraction order (usually = 1), G_A the grating area and F the focal length. Replacing Dl by its value as defined in equation (14), expression (16) becomes:

$$E_M = h\,Dx\ [D\,n\,k\,G_A\ /\ 10^6\,F] \tag{17}$$

where the parentheses term is for a given dispersing instrument (monochromator + grating) independent of the dimension of the entrance slit. Actually, one can demonstrate that this term is equal to the solid angle subtended by the monochromator entrance slit. Numerical values for Mcpherson scanning monochromator model 209 with a 1200 gr/mm grating [6]:

n (grating groove density)	1200 gr/mm	given
F (focal length)	1330 mm	given
f-number	11.6 (small grating)	given
D (dispersion)	0.62 nm/mm	given
G_A (grating area)	102 x 102 mm^2	given
h (slit height)	4 mm	chosen
Dx (slit width)	0.01 mm	chosen
W (solid angle)	5.83 x 10^{-3} steradian	calculated

Calculations using equation (12) yields:

$$E_M = (\,4\,) \bullet (\,0.01\,) \bullet (5.83 \times 10^{-3}) = 2.33 \times 10^{-4}\ mm^2$$

Calculations using equation (17) yields:

$$E_M = (4) \bullet (0.01) \bullet [(1200) \bullet (102)^2 \bullet (0.62) \bullet (1330)^{-1}\ (1 \times 10^6)^{-1}] = 2.33 \times 10^{-4}\ mm^2$$

One may argue that we should select a wider slit (both in terms of height and width) for the monochromator to increase the etendue. However, this solution has many drawbacks. Increasing the height of the slit will increase stray light that will affect both signal-to-noise ratio and resolution. Increasing the slit width will reduce the resolution of the instrument as stated in equation (14).

2.2 Optimization and matching

Matching a source to a monochromator will consist in selecting an optical system that will provide, coming from the plasma, a light beam that matches the geometric etendue of the instrument. In other words, the etendue of the entire system will be optimized if [1]:

$$E_o = E_M \tag{18}$$

If the optical etendue is larger than the instrumental etendue, then light will be wasted. Making the instrumental etendue greater than E_o will lead to a low light intensity in the spectrometer. Usually, the $E_o = E_M$ condition cannot be completely implemented since some considerations with

experimental hardware limitations takes precedent (example distance between plasma and spectrometer). These considerations will ultimately determine the effective etendue of the system. In order to obtain maximum light gathering sensitivity, one must attempt to provide a dispersing instrument that has an etendue approximately equal to the etendue of the light collecting system. Fulfillment of this condition will provide effective utilization of the light and optimization of the optical system.

2.2.1 Conventional optical system.

Let us examine how one must design the light collecting conventional optics to obtain a match between the monochromator and optical etendues. Examining equations (10) and (13), one can see that both etendues are proportional to the area of the monochromator slit. The only parameters that can be adjusted in the optics are the size, the magnification factor and the location of the lens. Choosing a 50 mm diameter lens, and replacing the numerical values for the slit height and width in equation (10), the optical etendue becomes:

$$E_o = S' A_L M^2 / X^2 = 78.5\, M^2 / X^2 \tag{19}$$

Let us now suppose that the plasma-lens distance is 1000 mm. This leads to the following condition for a match in the etendues: $M = (3)^{1/2} = 1.7$, which is easily achievable with a lens with a focal length of about 580 mm. A larger lens and a shorter distance increase the etendue. A series of solutions involving the three lens parameters (size, magnification factor, distance) are possible. Experimental limitations will dictate the selection of the lens. In this case the resolution of the spectroscopy system is determined by the monochromator.

2.2.2 Fiber optics system

The etendue of a fiber optics is given by [7]:

$$E_F = p\ S_f\ (NA_f)^2 \tag{20}$$

where NA_f and S_f are the numerical aperture and the cross-section area of the fiber optic, respectively. Choosing a fiber optics with a 50 μm diameter core and a 0.22 numerical aperture yields an etendue of 2.99×10^{-4} mm^2 which is about the same as the etendue of the monochromator (2.33×10^{-4} mm^2). However, if the fiber optics is simply inserted between the entrance slit jaws, the fiber numerical aperture (0.22) would drastically overfill the numerical aperture of the monochromator (0.043), both losing signal photons and creating stray light problems. The solution is to introduce a fiber optics adapter that will re-image the light emanating from the fiber in such a way that the numerical aperture of the fiber is brought down to that of the monochromator. This will permit a better capture and propagation of all available photons from the fiber through the monochromator. Let us define some parameters of the fiber optics adapter. We will consider that the fiber optic adapter has an entrance numerical aperture identified as NA_{in} and an exit numerical aperture identified as NA_{out}. The fiber optics adapter schematic is shown in Figure 4. The fiber optics enter the device on one end, while the monochromator slit acts as the aperture stop on the other side. The fiber optics adapter is composed of a Galilean telescope (also call beam expander) which consist of a matching pair of converging and diverging lenses (focal

length of each lens is located at the same point). Thus, the fiber optics adapter can increase or reduce the size of the beam to match the numerical aperture. In order to match the numerical aperture, the etendue of the system must remain the same:

$$E = p\, S\, (NA_{in})^2 = p\, S'\, (NA_{out})^2 \tag{21}$$

where S is the area of the fiber optics core and S' the area of the fiber core image. Equation (21) can be rewritten as:

$$(S'/S)^{1/2} = NA_{in} / NA_{out} \tag{22}$$

Since the numerical apertures of the fiber optics and monochromator are 0.22 and 0.043, a reduction by a factor of about 5 (magnification factor) in the aperture is needed at the expense of a larger image. Thus, the numerical aperture matching introduce a magnification of the image by a factor of 5. Although this solution results in an image of the fiber core that is larger than the slit width, it provides the best illumination and maximum throughput scenario. Since the fiber core image is now larger than the monochromator slit width (250 μm compare to 100 μm), the monochromator slit width must be increased to 250 μm at the expense of resolution. The slit height can be reduced by a factor of 2.5 to keep the monochromator etendue constant. At this point, the etendue are matched and all the light exiting the fiber optics will propagate though the monochromator. This means that the optimum slit width for best illumination (maximum throughput) is 250 μm. Increasing the slit width beyond 250 μm will serve no purpose (no illumination gain, increased stray light). Thus, if the image width of the fiber core is less than the slit width, the bandwidth of the spectrometer will be determined by the image of the fiber core instead of the slit width of the monochromator. This implies that the slit width should always be reduced to match the width of the fiber core image to minimize stray light.

Consequently, one could conclude that the width of the fiber core image at the fiber optics adapter should dictate the resolution of the monochromator. In reality, since the fiber optics do not transmit light uniformly over their entire cross-section, an improvement in resolution is expected when the slit width is reduced even beyond the fiber core image at the slit. Optimization is achieved by monitoring the resolution as a function of the slit width. Of course, any increase of resolution will be at the expense of intensity. Beyond a certain slit width (optimum width) no resolution improvement will be possible.

3.0 Spectroscopy Diagnostics

3.1 Line Emission and Photonic Current

We consider the spectroscopy system describe in Figure 5a. The plasma emits light that is collected by a collimator and sent through fiber optic to the spectrometer. Considering a specific transition ($l = k$) in a plasma, the emissivity term (watt/volume • solid angle) as defined in equation (4) can be written as:

$$e_k = (4p)^{-1}\, h n_k\, N_k\, A_k \tag{23}$$

Where $h\nu_k$ is the photon energy associated to the transition, N_k is the population of the emitting level (cm^{-3}) and, A_k is the Einstein coefficient for the transition (transition probability). Assuming that the plasma is uniform (the emitter density is uniform within the plasma volume) and, using equation (4), the photonic current (ampere) measured by a photomultiplier is given by [5]:

$$I_p(k) = (4p)^{-1} h\nu_k N_k A_k V W T_k Y_k \quad (24)$$

Where V is the plasma volume seen by the monochromator, W is the solid angle subtended by the collection optics, T_k is the transmission factor of the detection system and, Y_k (amp/Watt) is the sensitivity of the detector (photomultiplier). The sensitivity of the detector can be written as:

$$Y_k = h_k G e / h\nu_k \quad (25)$$

Where h_k is the quantum efficiency of the detector at wavelength k, G is the gain of the detector and, e is the unit of charge. For a CCD the expression is slightly different, the sensitivity being in count/Watt and the photonic current is in counts (one must drop the unit of charge term from the equation (25)). Replacing the expression for the sensitivity in equation (24) we have:

$$I_p(k) = (4p)^{-1} N_k A_k V W T_k h_k G e \quad (26)$$

For a given transition of wavelength k, the number of photons per second (line intensity) captured by the detection system can be written as:

$$I_k = (4p)^{-1} N_k A_k V W \quad (27)$$

The photonic current is related to the line intensity by:

$$I_p(k) = I_k (T_k h_k G e) \quad (28)$$

Where the last 4 terms are conversion factors to convert line intensity into photonic current. These terms can be evaluated by performing a calibration. In the case of a line ratio diagnostic a simple relative calibration is needed to evaluate the response of the spectrometer at different wavelengths. The complete procedure is described in Appendix A. In the case of the plasma specie density evaluation, an absolute calibration is needed to quantify the emitters in the plasma. Details can be found in Appendix B.

3.2 Excited Level Population

Although absolute numbers of the emitting level of the excited atoms or ions may sometimes be desirable, it is often more important to obtain information about the overall ion density or the electron temperature in the plasma. In order to link the excited level population to any of these quantities, a model must be used. A good discussion about the models that can be used to describe the different types of plasmas can be found in reference [5]. Basically for plasma conditions observed in Helicon sources, two models can be used. At lower electron density, ($n_e < 10^{12}$ cm^{-3} for He, lower for Ar) the simple Steady State Corona model can be used to predict the

population of the excited levels. Meanwhile, for higher plasma densities, the more complex Collisional Radiative Model is a better choice. Usually, both models can be used within a common range (10^{11} cm^{-3} < n_e < 10^{12} cm^{-3} for He) and calculated values can be compared.

3.2.1 Steady State Corona Model

According to McWhriter [5], the Steady Sate Corona (SSC) model can be used to predict the population of the excited levels provided the plasma conditions satisfy all of the applicability criteria for the model. For this model the following conditions must be valid: the electron velocity distribution can be described by a Maxwellian; the ion and neutral temperatures are less or equal than the electron temperature; the plasma is optically thin to its own radiation. The issue of plasma opacity has been studied in details in the WVU internal report: "Mean Optical Depth and Optical Escape Factor for Helium Transitions in Helicon Plasmas " [8]. The technique presented in this document can be adapted for different gases. It is consistent with the SSC model that only a small fraction of the neutral or ion populations are in one of their possible excited states with respect to their ground state. In this model, a balance between the rate of collisional excitation from the ground level and the rate of spontaneous radiative decay determines the population densities of the excited levels.

As a first step, let us assume that each line emission is the result of single collisions between electrons and atoms in the ground state and that all the applicability criteria for the model are satisfied. Under the SSC model, the population of the level j (N_j) is given by [5]:

$$n_e N_o <s\ v>_{oj} \quad = \quad N_j S_{i<j} A_{ji} \tag{29}$$

Where N_o is the population of the ground level population, n_e is the electron density, $S_{i<j} A_{ji}$ is the total transition probability from level j to all lower states and, $<s\ v>_{oj}$ is the excitation rate coefficient for the electron impact excitation of the level j from ground state. Thus, from the emitter population, provided one knows the excitation rate coefficient for this level and the different transition probabilities associated with this level, one can evaluate the neutral or the ion density. Isolating N_j in equation (29) as a function of the remaining terms and multiplying each side by A_{ji}, we obtain the emission rate (photons per unit volume and per second):

$$N_j\ A_{ji} \quad = \quad n_e N_o <\ s\ v\ >_{oj}\ A_{ji}\ (\ S_{i<j} A_{ji}\ )^{-1} \tag{30}$$

We introduce in equation (30) the "branching ratio" $B_{ji} = A_{ji}\ (S_{i<j}\ A_{ji}\ )^{-1}$ (unitless) which corresponds to the ratio of the transition probability of a specific from level *j* on the total transition probability from level *j*; expression (30) becomes:

$$N_j\ A_{ji} \quad = \quad n_e N_o <\ s\ v\ >_{oj}\ B_{ji} \quad = \quad n_e N_o E_{ji} \tag{31}$$

where $E_{ji} = B_{ji} <\ s\ v\ >_{oj}$ is the emission rate coefficient (photons x unit volume per second). Cross-sections for electron impact excitation from ground state to the different excited levels are used to evaluate the excitation rate coefficients. The cross-sections have been measured by a number of researchers (crossed-beam experiments) and a few compilations are available [9-12]. The excitation rate coefficient is defined as:

$$< s \;\; v > = \int_{-\infty}^{\infty} s \;\; v \;\; f(v) \;\; dv \qquad \text{(units in cm}^3 \text{ sec}^{-1}\text{)} \tag{32}$$

where the cross-section σ is averaged over the electron velocity distribution *f(v)*, assumed to be Maxwellian. The SSC model is believed to be able to predict the excited level populations with reasonable accuracy for electron density up to the mid-to-high 10^{11} cm^{-3}. At higher densities, secondary processes (excitation transfer between neighboring levels, excitation from metastables) are increasingly important, casting serious doubt on the validity of the SSC model to predict accurately predict these populations.

3.2.2 Secondary Processes

Up to now, we have assumed that the line emission is the result of single collisions between electrons and atoms in the ground state, followed by direct radiative de-excitation. At higher densities, this assumption is not valid because a number of secondary processes involving collisions with excited or ionized atoms is important. The secondary processes include: volume recombination (a fraction of the total recombination collisions induce the formation of one of the upper line levels); collisions between excited atoms and ground state atoms (by this mechanism a highly excited atom can lose part of its excitation to another atom in the ground state resulting in one or two more excited atoms; cascading redistribution effects (this process involves the electron impact excitation of a highly excited level followed by transition (s) to the upper line levels, excitation transfer collisions (the upper line levels can be populated or depopulated by excitation transfer collisions. Neighboring atomic levels are depleted or augmented with these collisions; excitation from metastables (the upper line levels can be excited through collisions between electrons and the metastable states of the atom).

First, let us examine helium plasmas. We limit this discussion to low temperature, low density He plasmas ($T_e \leq 20$ eV, $n_e \leq 1 \times 10^{13}$ cm^{-3}) as observed in HELIX plasmas where several of these secondary processes can be neglected. The effect of volume recombination is negligible since the recombination rate at these plasma densities is much smaller than the excitation rate. The effect of collisions between excited and ground atoms is negligible since the ion neutral collision time is much longer than the upper line de-excitation period. The cascading redistribution effect will be important if the electron temperature is comparable to the upper line level energy. Since the first excited level of the He atom is at 19.81 eV [13], this redistribution effect is negligible. The excitation transfer collisions effect will be important if the upper line level has neighboring level(s) with nearly the same energy. Excitation transfer cross-sections are also significantly larger when transitions between levels are optically allowed [14]. Finally, excitation from the metastable levels can be important, especially if these levels are close to the ground level (large metastable population) or that these metastable levels are energetically close to the excited levels responsible for the detected transitions.

Fortunately, excitation transfer contributions can be minimize by a proper selection of transitions, while contributions from the metastable levels can be evaluated with reasonable accuracy using the Collisional Radiative model prediction for the metastable populations (see next section) and the excitation rate coefficients from the metastable levels [11, 15-18]. These contributions can be included in the emission rate expression (equation 31) by replacing the emission rate coefficients by an apparent or resulting emission rate coefficient E_{ji}* that includes both direct (ground) and indirect (metastables) excitations:

$$N_j \; A_{ji} \; = \; n_e \, N_o \, E_{ji}^* \tag{33}$$

For Ar plasma, the situation is much more complex. Apart from the inherent complexity of this large atom (18 electrons), the presence of many low energy metastable states makes secondary excitation processes very important in the plasma even at low electron temperature [13, 19, 20]. Furthermore, the presence of a large ion population due to the low ionization energy threshold makes it very difficult to use the SSC model even in low density and low temperature plasmas. Thus, for Ar plasmas the Collisional Radiative model must be used for about all plasma conditions observed in HELIX. The database for the excitation rate coefficients for the different levels of the argon atom is less complete than the He database [11, 15-18]. Spectroscopy diagnostics for the Ar plasmas will be studied in a future document.

3.2.3 Collisional Radiative Model

A Collisional Radiative (CR) model can also be used to predict the population of the excited levels. The essential difference between the SSC model and the CR model is that the later model does not assume that bound excited populations originate exclusively from the ground state via electron impact excitation. In this model, secondary processes like excitation transfer, recombination and, ionization involving all excited states are included in the computation. In order to use this model, the plasma must satisfy the following conditions [5]: the electron velocity distribution can be described by a Maxwellian; the ionization process is by electron collision from any bound level and is partially balanced by three-body recombination into any level; excitation transfer between any pair of bound level are induced by electron collisions; radiation is emitted when a bound electron makes a spontaneous transition to a lower level or when a free electron makes a collisionless transition into abound level; the plasma is optically thin to its own resonance radiation. With these assumptions, a set of equations describing the population of bound levels N_i can be written as [5, 21, 22]:

$$dN_i/dt \; = \; n_e \, S_{j^1 i} \; S_{ji} \, N_j \; + \; S_{j>i} \; A_{ji} \, N_j - \; n_e \, S_{j^1 i} \; S_{ij} \, N_i \; - \; S_{j<i} \; A_{ij} \, N_i - \; n_e \, I_i \, N_i \; = \; 0 \tag{34}$$

The N_i values are both function of electron temperature and plasma density. The first term corresponds to the excitation or de-excitation of the electron population of all levels j that ends up at level i. The second term corresponds to the spontaneous de-excitation (allowed transitions) from higher j levels to level i. The third term is associated with the excitation or de-excitation of level i. The fourth term is the spontaneous de-excitation (allowed transitions) originating from level i. The last term is associated with the ionization rate of the electron population of level i. Each level of the atom is described by a similar equation. A system of N (level number) coupled differential equations must be solved simultaneously to obtain the population of a given level. For the He and Ar atom, the second and fourth terms on the right side of equation (34) can be evaluated with good accurately since the A_{ij} coefficients are well known [23, 24]. However, the picture is quite different for the remaining terms. Generally, the excitation (or de-excitation) cross-sections of short-lived excited state are poorly known (extremely difficult to measure). Theoretical calculations [15] are often used to fill the missing excitation rate coefficients. Cross-sections obtained by different models can vary by one or more order of magnitude at low electron

energy [15]. Again, the He excitation transfers database for He although poor is by far better than the Ar database.

3.3 Ion/Neutral Density Diagnostic

To evaluate the ion or neutral density from the plasma radiation, one must first proceed with an absolute calibration of the spectroscopy system (Appendix B). In this case, the known emissivity of the calibrated lamp is used to evaluate the emitters density responsible for the studied transition. Again, the photonic current associated with a plasma emitter density N_k is given by:

$$I_p(k) = (4p)^{-1} N_k A_k V W T_k h_k G e \tag{26}$$

Similarly, the photonic current associated to the calibrated source (optical path described in Figure 5b) at the same wavelength is given by:

$$I_{cs}(l_k) = e_k(d)\, l_k (hc)^{-1} S D l T_k h_k G e \tag{A-1}$$

Where $e_k(d)$ is the calibrated lamp emissivity at wavelength k and at the calibration distance d (d = 0.5 m) (units in Watt m^{-2} nm^{-1}), and S is the optics collecting area. Utilizing the fact that apart from the source section, both optical paths are the same, the emitter density is linked to the detected photonic current by the expression (see Appendix B):

$$N_k A_k = F_{abs} I_p(k) \tag{B-5}$$

Where the absolute calibration factor F_{abs} (cm^{-3} sec^{-1} amp^{-1}) is given by:

$$F_{abs} = \frac{4p\ l_k e_k R^2 \Delta l\ S}{d^2\ V\ hc\ I_{cs}(k)} \tag{B-6}$$

Combining equations (31) and (B-5) and using the notation $ji = k$, the neutral density can be written as:

$$N_o = F_{abs} I_p(ji) (n_e B_{ji} < s\, v >_{oj})^{-1} = F_{abs} I_p(ji) (n_e E_{ji})^{-1} \tag{35}$$

The neutral density is thus a function of all the following parameters: detected photonic current, electron density, excitation rate coefficient for this emitting level, branching ratio. Similarly, for the ion density and, looking at a transition between level m and n we have:

$$N_i = F_{abs} I_p(mn) (n_e E_{mn})^{-1} \tag{36}$$

Again, we assumed that the line emission is the result of single collisions between electrons and atoms in the ground state, followed by direct radiative de-excitation. Replacing the excitation rate coefficient by an apparent or resulting emission rate coefficient that includes both direct excitation and the indirect excitation can takes into account secondary processes. Using this new excitation coefficient, the expression (35) becomes:

$$N_o = F_{abs}\ I_p(ji)\ (n_e\ E_{ji}^*)^{-1} \tag{37}$$

Similarly, for the ions, equation (36) becomes:

$$N_i = F_{abs}\ I_p(mn)\ (n_e\ E_{mn}^*)^{-1} \tag{38}$$

3.4 Line Ratio Diagnostic (Electron Temperature Diagnostic)

The line ratio diagnostic is based on the fact that the dependence on the electron energy of the cross-sections for excitation by electron impact differs between two lines of neutral atoms (or ion). The electron temperature in an experiment is calculated from measured line intensities by the use of excitation cross-sections obtained in crossed beam experiments. Again, in a first step, it is assumed that the line emission is the result of single collisions between electrons and atoms in the ground state, followed by direct radiative de-excitation. The secondary processes will then be included by the same method described in the previous section. Considering two lines at wavelength *k* and *j* for the diagnostic. The ratio of the photonic current is according to equation (26) given by:

$$\frac{I_p(k)}{I_p(j)} = \frac{I_k\ T_k\ h_k\ G\ e}{I_j\ T_j\ h_j\ G\ e} \tag{39}$$

In this case only a relative calibration of the spectroscopy system. According to Appendix A, the photonic current ratio can also be expressed as:

$$\frac{I_p(k)}{I_p(j)} = \frac{1}{F_R}\frac{I_k}{I_j} \tag{A-5}$$

where F_R is the relative calibration factor. Using equation (26), the expression (A-5) becomes:

$$\frac{I_p(k)}{I_p(j)} = \frac{1}{F_R}\frac{N_k A_k}{N_j A_j} \tag{40}$$

Replacing the emitter densities by using equation (30) and using the definition of the branching ratio the equation (40) becomes:

$$R_I(T_e) = \frac{I_p(k)}{I_p(j)} = \frac{1}{F_R}\frac{< sv >_{ok}\ B_k}{< sv >_{oj}\ B_j} \tag{41}$$

where $R_I(T_e)$ is the line ratio function which depends solely on the electron temperature. Thus, the ratio of the photonic currents (observable quantities) can be linked to the electron temperature in the plasma. Up to now, we assumed that the line emission is the result of single collisions between electrons and atoms in the ground state, followed by direct radiative de-excitation. In reality the

ratio may depends on the electron density because of the secondary excitation process defined in the previous section. Again, by using the resulting emission rate coefficients E_k* and E_j*, the line ratio becomes:

$$R_I(T_e) = \frac{I_p(k)}{I_p(j)} = \frac{1}{F_R}\frac{E_k^*}{E_j^*} \tag{42}$$

Other spectroscopic measurements are possible but they will not be presented in this document. Each of these more complex techniques will be reviewed in separate internal reports.

3.6 Oriel Model QTH 200W Calibration Curve.

The calibration curve of the Oriel's Quartz Tungsten Halogen lamp Model QTH 200W is given in Figure 5. The irradiance data comes from Oriel Calibration Datasheets [25]. The irradiance $I(l)$ (in mWatt/m^2 nm) at different wavelength can be calculated by using the fitting equation [25]:

$$I(l) = l^{-5}\,[\exp(A + B/l)] \times (C + D/l + E/l^2 + F/l^3 + G/l^4 + H/l^5) \tag{43}$$

With the following parameters:

A = 4.30583 x 10^1	E = 4.98368 x 10^5
B = - 4.60203 x 10^3	F = - 2.76490 x 10^8
C = 1.05104 x 10^0	G = 6.80661 x 10^{10}
D = - 3.39311 x 10^2	H = - 6.35625 x 10^{12}

Irradiance tables are also available from the Oriel Calibration Datasheets [23]. These tables gives the irradiance at every 100, 10 and 1 nm (Oriel diskette, ASCII format). The source was calibrated with a reference NIST source [26]. The uncertainty is the quadratic sum of the source precision and the NIST uncertainty. The uncertainty at different wavelengths is given in table 1. The uncertainty is smallest in the 350 to 1300 nm range.

Table 1. Irradiance uncertainty at different wavelengths for the QTH 200W lamp.

Wavelength (nm)	250	350	654.6	900	1300	1600	2000	2400
Uncertainty (%)	2.7	1.85	1.75	1.85	1.88	2.45	3.07	4.87

Appendix A Relative Calibration

Before using a line ratio diagnostic to evaluate the electron temperature of the plasma, one must calibrate the spectrometer as a function of wavelength. Since this diagnostic is based on a line ratio technique, only a relative calibration is needed. Let us consider the second optical path shown in Figure 6b. The plasma is replaced by a calibrated tungsten source while the rest of the optical path is exactly the same. The photonic current associated with this lamp at the wavelength l is given by the expression:

$$I_{cs}(l) = e_l(d)\, l\, (hc)^{-1}\, A\, D l\, W\, T_l\, h_l\, G\, e \tag{A-1}$$

Where $e_l\ (d)\ l\ (hc)^{-1}$ is the spectral irradiance of the lamp (also called lamp emissivity, units: photons steradian^{-1} cm^{-2} nm^{-1} sec^{-1}) at a distance d from the lamp filament ($e_l\ (d)$ is in Watt steradian^{-1} cm^{-2} nm^{-1}). A is the optic collecting surface seen by the monochromator and $D l$ is the bandwidth. The photonic conversion factors can be written as:

$$T_l h_l Ge = \frac{I_{cs}(l)hc}{l e_l(d)A\Omega\Delta l} \tag{A-2}$$

Considering two lines at wavelength *k* and *j* for the diagnostic. The ratio of the photonic factors for the 2 transitions is equal to:

$$\frac{T_k\, h_k\, G\, e}{T_j\, h_j\, G\, e} = \frac{I_{cs}(k)\ e_j(d)\ l_j}{I_{cs}(j)\ e_k(d)\ l_k} \tag{A-3}$$

Replacing this expression in equation (28) the photonic current ratio becomes:

$$\frac{I_p(k)}{I_p(j)} = \frac{I_k}{I_j}\ \frac{I_{cs}(k)e_j(d)l_j}{I_{cs}(j)e_k(d)l_k} \tag{A-4}$$

Thus, the line intensity ratio can be written as:

$$\frac{I_k}{I_j} = F_R\, \frac{I_p(k)}{I_p(j)} \tag{A-5}$$

with F_R as the relative calibration factor for *k* and *j* line and is given by:

$$F_R = \frac{I_{cs}(j)e_k(d)l_k}{I_{cs}(k)e_j(d)l_j} \tag{A-6}$$

Since $I_{cs}(l)$ changes monotonically with l, one can see that if *k* is almost the same as *j*, the factor is close to unity. The measure of the relative calibration factor is straightforward, one must measure the response of the spectrometer at the two chosen wavelengths with the calibration lamp and use equation (A-6) to evaluate the factor F_R.

Appendix - B Absolute calibration

For ion density measurement, relative calibration is insufficient. The calibrated emission of the calibration source is used to evaluate the number of emitters. Again, the conversion factors (as identified in equation (8)) associated with photonic current of the plasma emitters are given by:

$$T_k \, h_k \, G \, e \;=\; 4p \, I_p \, (k) \;\; (N_k \, A_k \, V \, W)^{-1} \tag{B-1}$$

Similarly, the conversion factors associated with the photonic current of to the calibrated source at the same wavelength is given by:

$$T_k \, h_k \, G \, e \;=\; I_{cs} \, (l_k) \, hc \, (e_k \, (d) \;\; l_k \, S \, W \, D \, l)^{-1} \tag{B-2}$$

Since the optical path is the same in both setups, the number of photons per second and by unit volume ($N_k \, A_k$) can be written as:

$$N_k A_k = \frac{4p \;\; l_k e_k \, (d) \Delta \, l \;\; S}{V \;\; hc} \;\; \left(\frac{I_p \, (k)}{I_{cs} \, (k)}\right) \tag{B-3}$$

Often, the lamp calibration is given at a distance (R) different that the one used in the experimental setup (d). Providing that the distance d is larger than 20 to 30 times the radiating filament, the irradiance will follows the inverse square law [26]. In our case, the filament size is approximately 0.7 by 0.35 cm^2. Since the collecting optics is located at 20.7 cm from the plasma center (or the lamp filament) the condition is fulfilled. Thus, the spectral radiance of the lamp at the distance d and for any given wavelength within the emission spectrum is given by:

$$e_l \, (d) \;=\; e_l \, (R/d)^2 \tag{B-4}$$

Replacing the expression for spectral radiance in the previous equation we obtain:

$$N_k \, A_k = \frac{4p \;\; l_k e_k R^2 \Delta \, l \;\; S}{d^2 \;\; V \;\; hc} \;\; \left(\frac{I_p \, (k)}{I_{cs} \, (k)}\right) = F_{abs} \, I_p \, (k) \tag{B-5}$$

The absolute calibration factor that converts photonic current in the emitter density times the emission probability is given by:

$$F_{abs} \;=\; \frac{4p \;\; l_k e_k R^2 \Delta \, l \;\; S}{d^2 \;\; V \;\; hc \;\; I_{cs} \, (k)} \tag{B-6}$$

References:

[1] Bousquet P., "Spectroscopie Instrumentale". Dunod (1969)
[2] Turner B., Optical and Ultraviolet Techniques, in Plasma Diagnostics Techniques, Chap. 7, Academic Press (1965)
[3] DeSilva A. W. and G. C. Goldenbaum, Plasma Diagnostics by Light Scatttering, in Methods of Experimental Physics: Plasma Physics Part A, Chap. 3, Academic Press (1970)
[4] Lochte-Holtgreven W. and J. Richter, Quantitative Spectroscopy and Spectral Photometry, in Plasma Diagnostics, Chap. 5, North-Holland (1968)
[5] McWhirter R. W. P. Spectral Intensities, in Plasma Diagnostic Techniques, Chapter 5, Academic Press, (1965)
[6] McPherson, Instruction Manual for the Model 209 1.33 Meter Scanning Monochromator (1998)
[7] ISA Jobin Yvon, SPEX, Guide for Spectroscopy (1999)
[8] Boivin R. F., Mean Optical Depth and Optical Escape Factor for Helium Transitions in Helicon Plasmas. WV-PL-045, West Virginia University, (2000)
[9] De Heer F.J. et al., Nucl. Fusion Suppl. **3**, 19 (1992)
[10] Trajmar S., Electron Collision Processes with Plasma Edge Neutrals, Nucl. Fusion Suppl. V.2 IAEA (1992)
[11] Kato T., Y. Itikawa and K. Sakimoto, NIFS-DATA-15 (1992)
[12] Kato T. and R.K. Janev. Nucl. Fusion Suppl. **3**, 33 (1992)
[13] Moore C. E., Atomic Energy Levels, Vol 1, Natl. Bur. Stds., NSRDS-NBS 35 (1971)
[14] Brenning N. J.Quant. Spectrosc Radiat. Transfer **24**, 319 (1980)
[15] Shevelko V. P. and H. Tawara, NIFS-DATA-28 (1995)
[16] Goto M. and T. Fujimoto, NIFS-DATA-43 (1997)
[17] Trajmar, S., D.F. Register and A. Chutjan, Physics Reports **97**, 219 (1983)
[18] Trajmar, S. and D.C. Cartwright in Electron Molecule Interaction and their Application, Academic Press (1984)
[19] Rundel R. D. and R. F. Stebbings, The Role of Metastables Particles in Collision Processes in Case Studies in Atomic Collision Physics II. Chap. 8, North Holland (1972)
[20] Bashkin S. and J.O. Stoner, Atomic Energy Levels and Grotrian Diagrams, V. 2, North Holland (1975)
[21] Brosda B. Ph.D. Thesis, Ruhr-Universitat, Bochum (1993)
[22] Sasaki S., S. Takamura, S. Masuzaki et al., NIFS-346 (1995)
[23] Theodosiou C.E., At. Data Nucl. Data Tables **36**, 97 (1987)
[24] Wiese W. L., M. W. Smith, and B. M. Glennon, Atomic Transition Probabilities, Vol.1. National Standard Reference Data Series (1966)
[25] Oriel Instruments, Report of Calibration of One Standard of Spectral Irradiance (250 - 2400 nm) (1999)
[26] Oriel Instruments, Instruction Manual, Quartz Tungsten Halogen Lamp Standards of Spectral Irradiance (1996)

Figure 1. Czerny-Turner Monochromator

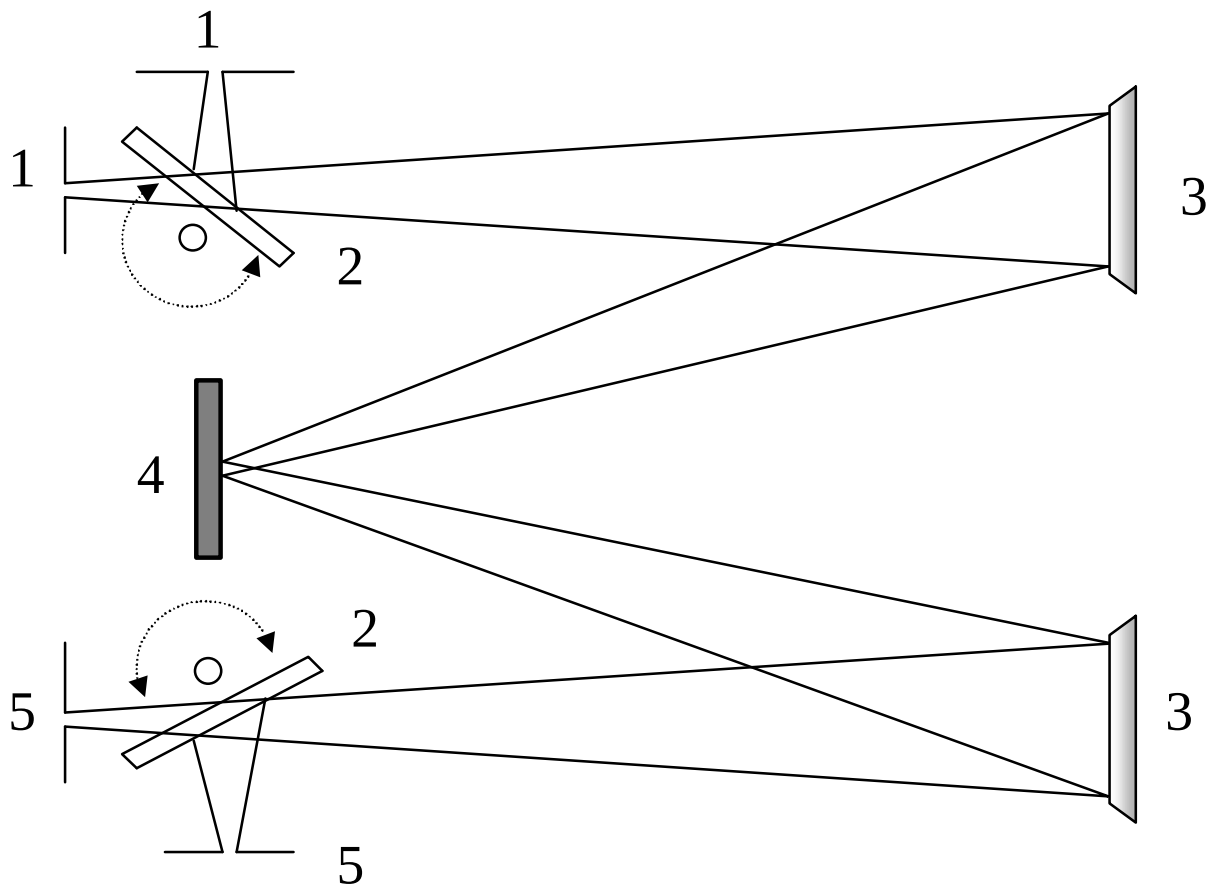

1: Entrance slits, 2: Folding mirrors, 3: Concave mirrors, 4: Grating, 5: Exit slits

Figure 2. Spectroscopy Defined Volume

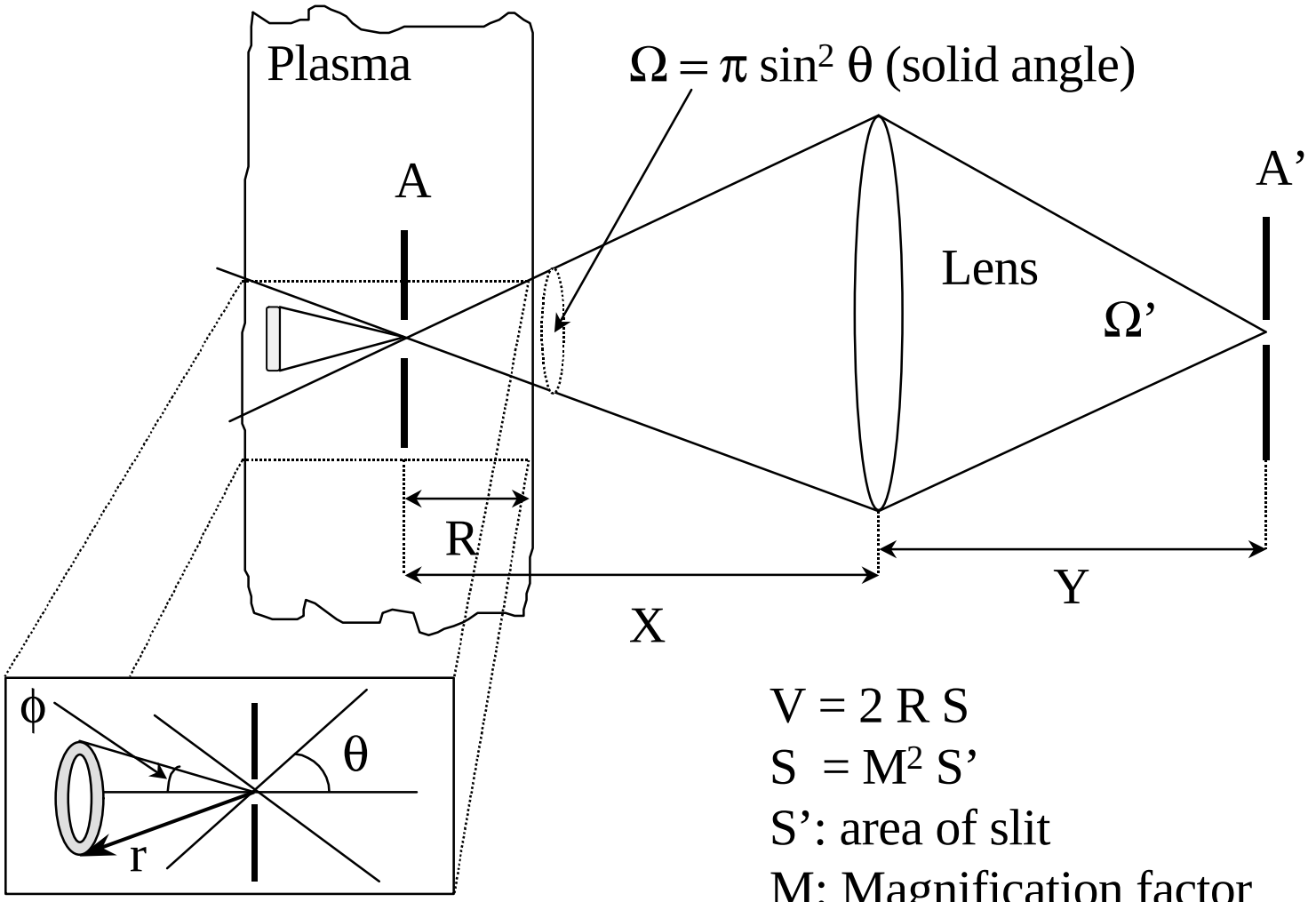

$V = 2 R S$

$S = M^2 S'$

S': area of slit

M: Magnification factor

Figure 3. Monochromator f-number

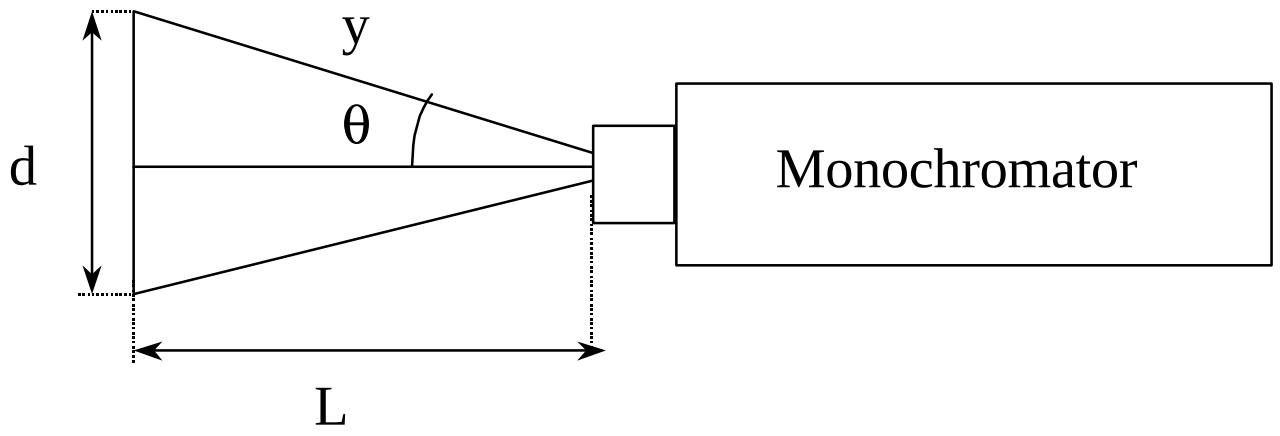

By definition we have: $f = L / d$

$\sin \theta = d / 2\, y$ with $y^2 = (d/2)^2 + L^2$

$\sin^2\theta = (1 + 4L^2/d^2)^{-1}$

$\sin^2\theta = (1 + 4f^2)^{-1}$

Figure 4. Fiber optics adapter (telescope)

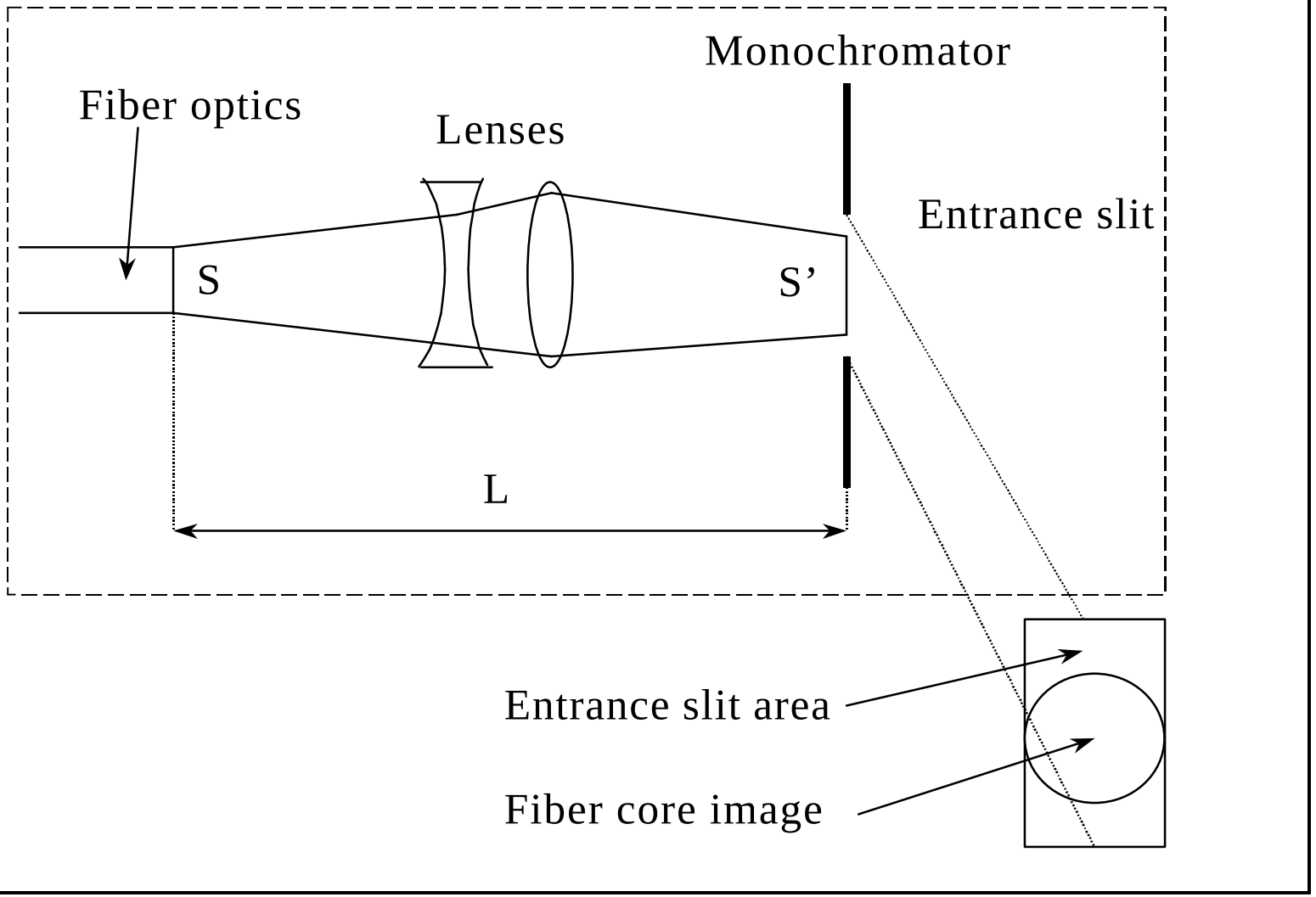

Figure 5. Calibration Lamp Irradiance

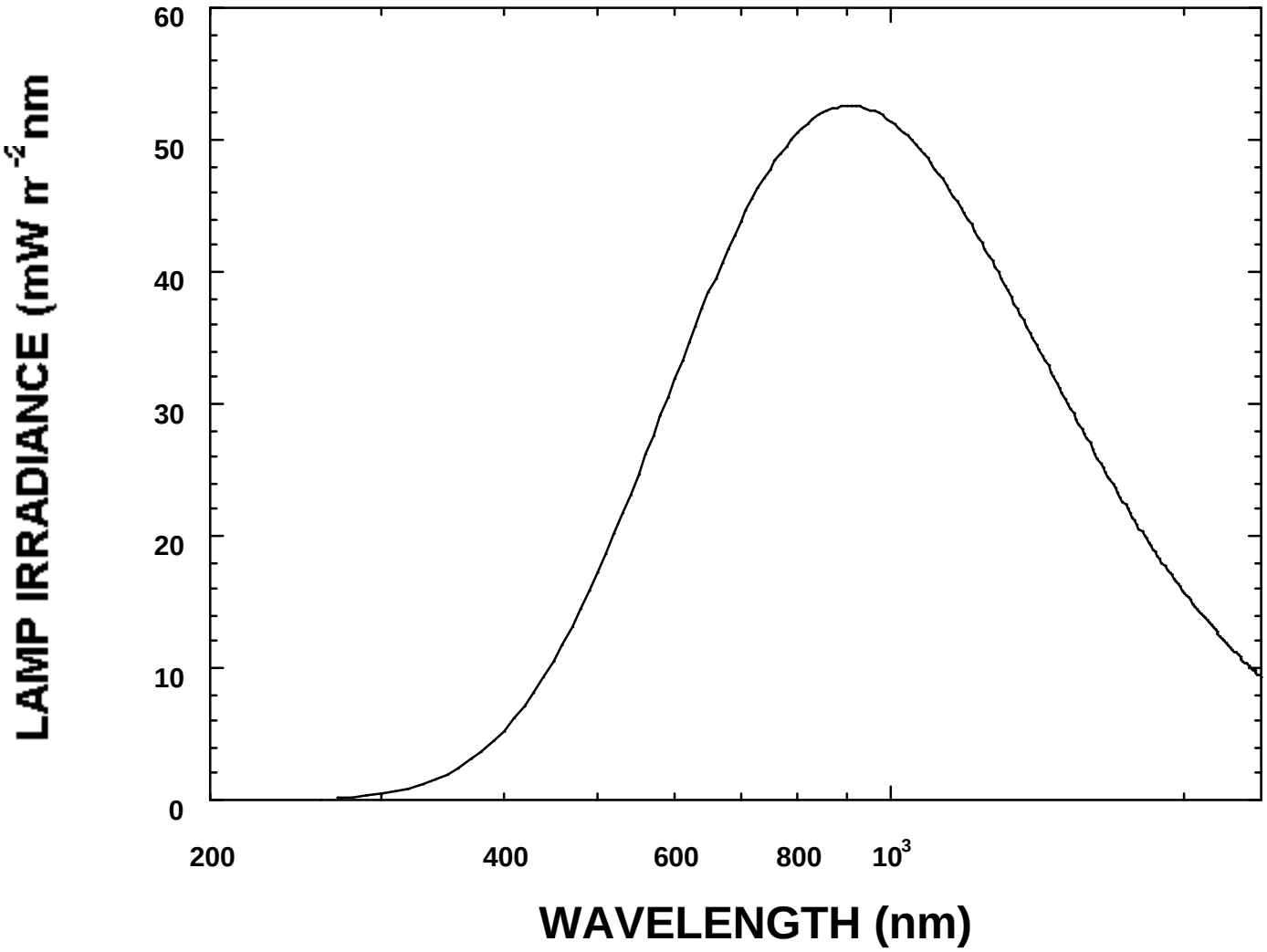

Figure 6. Calibration Setup

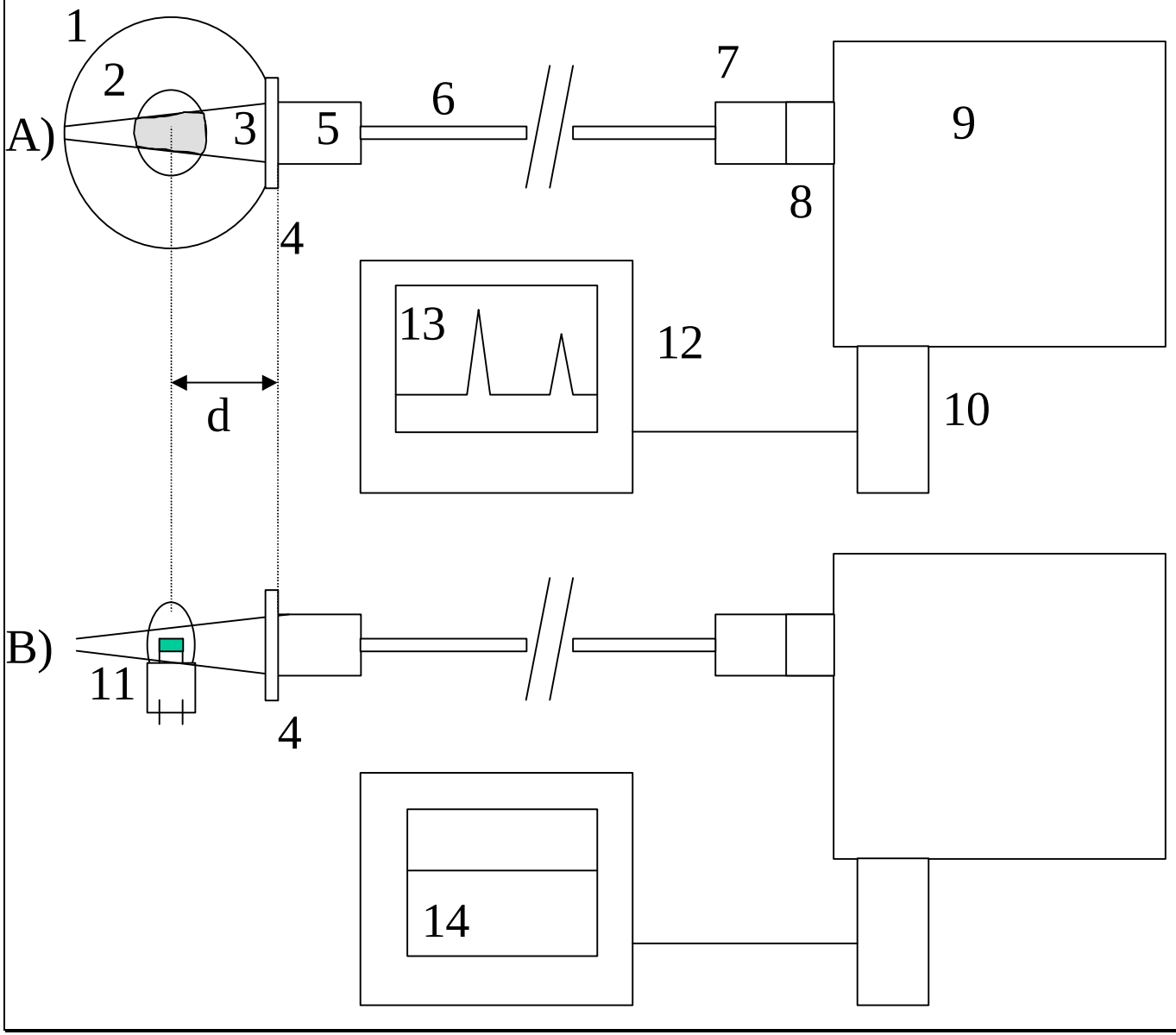

1- Chamber
2- Plasma Column
3- Solid angle
4- Viewport
5- Collimator
6- Fiber optics
7- Telescope
8- Entrance slit
9- Monochromator
10- CCD Camera or photomultiplier
11- Tungsten lamp
12- Computer
13- Discrete spectrum
14- Continuous spectrum